 doi:10.20944/preprints202012.0582.v1

Article

Liquid-based 3D Cultured Tumoroids Modeling Resistance to Cisplatin and Imatinib in Metastatic Colorectal Cancer

Chiharu Sogawa [1], Takanori Eguchi [1,2,*], Yuri Namba [1,3], Eriko Aoyama [2], Kazumi Ohyama [1], and Kuniaki Okamoto [1]

[1] Department of Dental Pharmacology, Okayama University Graduate School of Medicine, Dentistry and Pharmaceutical Sciences, Okayama 700-8525, Japan; kohyama@md.okayama-u.ac.jp (K.Oh.); k-oka@okayama-u.ac.jp (K.Ok.)

[2] Advanced Research Center for Oral and Craniofacial Sciences (ARCOCS), Okayama University Graduate School of Medicine, Dentistry and Pharmaceutical Sciences, Okayama University, Okayama 700-8525, Japan; eaoyama@md.okayama-u.ac.jp (E.A.)

[3] Department of Oral and Maxillofacial Radiology, Okayama University Graduate School of Medicine, Dentistry and Pharmaceutical Sciences, Okayama 700-8525, Japan; pon48yol@s.okayama-u.ac.jp (Y.N.)

* Correspondence: eguchi@okayama-u.ac.jp (T.E.); Tel.: +81-86-235-6662

Abstract: Researchers have developed and used several three-dimensional (3D) culture systems, including spheroids, organoids, and tumoroids. Drug resistance is a crucial issue involving recurrence in cancer patients. Many studies on anticancer drugs have been done in 2D culture systems, whereas 3D cultured tumoroids have many advantages for assessing drug sensitivity and resistance. Here, we aim to investigate whether Cisplatin (a DNA crosslinker), Imatinib (a multiple tyrosine kinase inhibitor), and 5-Fluorouracil (5-FU: an antimetabolite) alter tumoroid growth of metastatic colorectal cancer (mCRC). To establish a liquid-based 3D multiplexing reporter assay system, LuM1 (a murine mCRC cell line) was stably transfected with the *Mmp9* promoter-driven ZsGreen reporter gene, which was designated as LuM1/m9 cells and cultured in NanoCulture Plate (NCP), a 3D culture device. The larger tumoroids were not sensitive to Cisplatin and expressed ABCG2 (a marker of cancer stem cells, a.k.a. a drug efflux transporter), whereas smaller cell-aggregates were more sensitive to Cisplatin. Both Imatinib and Cisplatin significantly increased tumoroid growth (larger than 300 μm^2) and Mmp9 promoter activity and were not cytotoxic to the mCRC tumoroids. On the other hand, 5-FU was cytotoxic to the tumoroids and significantly inhibited tumoroid growth, although not completely. Thus, platinum resistance and imatinib resistance in mCRC were modeled using the liquid-based 3D cultured tumoroid system. The tumoroid culture is useful and easily accessible for the assessment of drug sensitivity and resistance.

Keywords: Liquid-based 3D culture; tumoroid; cisplatin resistance; imatinib (gleevec); tyrosine kinase inhibitor (TKI); organoid; spheroid; metastatic colorectal cancer (mCRC)

1. Introduction

The methodology of cell culture and tissue culture is essential in biology and medicine. Researchers have developed and used several three-dimensional (3D) culture systems, including colony formation assay [1], spheroids [2,3], organoids [4,5], and tumoroids [6,7]. There are several advantages of 3D culture than 2D culture: (1) The 3D cultured cells, tissues, organoids, and tumoroids are morphologically more similar to 3D tissues, organs, or tumors in the bodies. Organs and tumors developed in 3D culture systems obtain 3D structures with intercellular adhesion in vitro [6,7]; (2) 2D culture systems force attachment of tissues/cells on plastic plates induces forced integrin expression required for the attachment. There is no forced attachment in 3D culture systems. Instead, intercellular adhesion is formed among cells to form organ-like or tumor-like structures in the 3D culture systems [7]; (3) Cell cycle and cell growth in 3D culture systems resemble those in organs, tissues, or tumors in the bodies. Cells proliferate rapidly in 2D culture, whereas

 doi:10.20944/preprints202012.0582.v1

cells grow more slowly in 3D culture [7]. Slow cycling cancer cells, dormant cancer cells at the G0 phase, and cancer stem cells (CSCs) can cause low chemosensitivity, drug resistance, and relapse [8-11]. These slow and dormant cells are reconstructed in 3D tumoroids, which are accessible by researchers. Dormant cells are not chemosensitive but can be resistant against cell-cycle-dependent chemotherapeutics such as mitotic inhibitors, including taxanes and vinca alkaloids, topoisomerase inhibitors, and antimetabolites, including methotrexate and 5-fluorouracil (5-FU); (4) Liquid-based 3D culture systems are especially useful for adding and analyzing substances such as growth factors [12], drugs [13,14], and extracellular vesicles (EVs) [6,12,15] in the culture supernatants; (5) Organoids and tumoroids have been developed recently, more similar with organs and tumors, respectively, in the bodies than spheroids. In organoids and tumoroids, complicated structures of organs and tumors can be reconstructed in vitro. For example, tumor microenvironment such as vasculatures [16,17], immune cells [12], fibroblastic stromal cells, and normal epithelial cells can be reconstructed in vitro within organoids and tumoroids [18-20]; (6) Gene expression signatures, molecular profiles, and secretory phenotypes are particular in 3D tumoroids according to their physical properties, e.g., moonlighting metalloproteinases (MMPs) [6,13,21-23], ATP-binding cassette (ABC) transporters including ABC-G1 and ABC-G2 [15], and intercellular adhesion molecules such as EpCAM/CD326 and E-cadherin [7,12], stem cell markers such as CD44 variants and CD133 [7], other factors potentially involving stemness such as ESRP1/2, MUC1, and Notch/delta signal [7]. The molecular profiles of tumoroids involve properties of CSCs [7]. Of note, ABCG2 (a.k.a. breast cancer resistant protein (BCRP)) transports anticancer agents such as irinotecan, 7-ethyl-10-hydroxycamptothecin (SN-38), gefitinib, Imatinib, methotrexate, and mitoxantrone from cells [24].

Drug resistance is a crucial issue in cancer, which occurs recurrence or relapse in cancer patients. Some chemoresistance has been overcome; however, recent studies clarified resistance against molecularly targeted therapeutics, including antibody drugs [25,26]. Many studies on drug resistance have been done in 2D culture systems, whereas we recently have examined chemosensitivity and chemoresistance in the liquid-based 3D cultured tumoroids [13,14]. For example, 5-FU, an antimetabolite inhibiting DNA replication, inhibited tumoroid growth of metastatic colorectal cancer (mCRC), while this agent did not inhibit metastatic metalloproteinase activity of mCRC cells [14]. On the other hand, cortisol, an anti-inflammatory steroid hormone agent, inhibited metalloproteinase activity of the mCRC, whereas this agent did not inhibit but rather promoted tumoroid growth [14]. Moreover, using the liquid-based 3D culture system, we have identified repurposing drugs for cancer therapy: (1) artesunate, an anti-malaria drug, inhibits tumoroid growth of mCRC [14]; (2) benztropine, an anti-Parkinson disease drug, inhibits tumor growth and metastasis of mCRC [13].

However, chemosensitivity and chemoresistance are not fully investigated in 3D culture systems. DNA crosslinkers such as cisplatin and tyrosine kinase inhibitors (TKI) such as Imatinib (Gleevec) have not been well examined in 3D tumoroid culture systems. It is also not well studied whether 5-FU, a cell-cycle-dependent antimetabolite, is effective to tumoroids that include slow cycling, dormant cancer cells. Thus, in the present study, we aim to investigate whether Cisplatin, Imatinib, and 5-FU alter tumoroid growth of metastatic cancer cells in the liquid-based 3D culture system, which can model a new system for analysis of chemoresistance and chemosensitivity.

2. Materials and Methods

2.1. Cells and 3D culture

A murine colorectal cancer cell line Colon26 and its rapidly metastatic subline LuM1 were used [22,27,28]. LuM1/m9 reporter cells were established by the stable transfection of a murine *Mmp9* promoter (588 bp)-driven ZsGreen reporter construct into LuM1 cells [13,14]. These cell lines were maintained in RPMI 1640 containing 10% FBS supplemented with penicillin, streptomycin, and amphotericin B.

 doi:10.20944/preprints202012.0582.v1

For liquid-based 3D culture, LuM1/m9 cells were cultured using 96-well NanoCulture Plate (NCP) in RPMI 1640 medium supplemented with 2 or 10% FBS or mTeSR1 stem-cell medium (Stemcell Technologies, Vancouver, BC, Canada) as described previously [7,14].

2.2. Chemicals and drugs

Cisplatin (CDDP: cis-diamminedichloro-platinum(II)) and 5-FU were purchased from Wako (Osaka, Japan). Imatinib was purchased from Focus Biomolecules (Plymouth Meeting, PA).

2.3. Drug treatment

For analysis of in vitro tumorigenesis and chemoresistance, cells were seeded at a concentration of 5×10^3 or 1×10^4 cells per well in a 96-well NCP and then pre-cultured in mTeSR1 for 1, 3, or 4 days. Cisplatin was added to the pre-formed tumoroids at 10 μM, tumoroids were cultured 24 hours before viability assay. LuM1/m9 cells were seeded at 5×10^3 cells/well in a 96-well NCP and then cultured in 10% FBS-containing RPMI 1640 medium for 72 h with or without drugs (Cisplatin, Imatinib, or 5-FU) in the other experiments. After each drug's treatment, the size and viability of cell aggregate/tumoroid were measured as described below.

2.4. 3D Tumoroid-based multiplex reporter assay

Tumoroids of LuM1/m9 cells were formed in NCP as described above and previously [7,13,14]. The fluorescent area of each tumoroids or cell aggregates were analyzed using the ArrayScan HCS System (ThermoFisher Scientific, Waltham, MA). Fluorescent areas greater than 300 μm^2 were considered as tumoroids. *Mmp9* promoter activity was evaluated by an average fluorescence intensity per μm^2 of all cells in a well. Experiments were performed with 3 or 4 biological replicates.

2.5. Cell viability assay

The ATP content was quantified using a CTG luminescent cell viability assay (Promega, Medison, WI). Briefly, from the total 200 μl of culture supplement, 150 μl was removed, and 50 μl of CTG solution was added to each well and then suspended. The plate was rocked for 2 min and incubated for 10 min at 37°C. The luminescence was measured in a plate reader (Molecular Devices, San Jose, CA).

2.6. Side population cell analysis

Cells cultured on a 10-cm dish were washed with warmed PBS (-), detached using 5 ml of Accutase (Innovative Cell Technologies, San Diego, CA), and neutralized with 5 ml of the serum-contained medium. Cells were collected by centrifugation at 250 × *g* for 3 min and suspended in the serum-contained medium. Cell aggregates were removed by using a 35-μm cell strainer. The density of cells was adjusted to 10^6 cells/ml by adding the serum-contained medium. Cells were incubated at 37°C by using a water bath, mixed with Hoechst 33342 (ThermoFisher Scientific) at a final concentration of 5 μg/ml and/or verapamil (Sigma) at a final concentration of 30 μg/ml, and then incubated at 37°C for 90 min in a dark condition with stirring every 20 min. Cells were then centrifuged at 250 × *g* for 3 min and washed with ice-cold PBS (-) containing 2% FBS. The cell density was adjusted to 10^7 cells/ml and mixed with Propidium Iodide (PI) at a final concentration of 0.5 to 1.0 μg/ml. Cell aggregates were removed using the cell strainer, and single cells were analyzed using a FACSCalibur (BD Biosciences, Franklin Lakes, NJ) at Central Research Laboratory, Okayama University Medical School.

2.7. RT-qPCR

RT-qPCR was performed as described [13,15]. LuM1 cells were cultured in 2D or 3D conditions for 4 days, and total RNA was extracted using the AGPC method with Trizol (Molecular Research Center, Cincinnati, OH). cDNA was synthesized using ReverTra Ace (Toyobo, Osaka, Japan). Real-time PCR was carried out using iQ cyber (BioRad). Primers for *Abcg2* and *Hprt1* (an internal control) were listed in the previous report [15]. Relative

 doi:10.20944/preprints202012.0582.v1

levels of *Abcg1* mRNA to *Hprt1* mRNA were quantified by the ΔΔCt method using the formula as follows: fold change = $2^{-\Delta\Delta Ct}$.

2.8 Statistical analysis

Data were expressed as the means ± SD unless otherwise specified. Statistical significance was calculated using GraphPad Prism (La Jolla, CA). Three or more mean values were compared using one-way analysis of variance with the pairwise comparison by Turkey's method, while two were made with an unpaired student's *t*-test. $P<0.05$ was considered to indicate statistical significance.

3. Results

3.1. Tumoroids acquired platinum-resistance with ABCG2 expression in metastatic colorectal cancer cells

We have shown that the mCRC cell line LuM1 expressed a high level of ABCG2, drug efflux pump expressed in CSCs, than the milder colorectal cancer cell line Colon26 [15]. To evaluate platinum resistance and cancer stem phenotype of the mCRC cell line LuM1, we first examined whether the rate of side population (SP) cells was reduced by verapamil, an ABCG2 inhibitor. The rate of SP cells in untreated LuM1 cells was 7.8%, while verapamil reduced it to 2.2%, suggested that this mCRC cell line contained ABCG2+ CSCs (Figure 1A). The rate of SP cells in Colon26 was 2.9%, thus fewer than that of LuM1, while verapamil further reduced the SP cells in Colon26 down to 0.4% (Figure S1).

Next, we examined whether the mCRC cells' platinum resistance was altered by 2D vs. 3D culture systems, the size of tumoroids, and the type of liquid environments (serum vs. stemness enhancing medium). The NCP-based 3D culture condition promoted tumoroid growth compared with a 2D culture system (Figure 1B, C). Stemness enhancing medium (mTeSR1) also promoted tumoroid growth compared to the serum-contained medium. Cisplatin reduced cell viability (ATP activity) in 2D culture conditions and in the serum-contained medium. In contrast, the cytotoxicity of Cisplatin was reduced by larger tumoroid formation based on the 3D culture system and the stemness-enhancing medium. Notably, the combination of the 3D culture and mTeSR1 markedly promoted cisplatin-resistant tumoroid growth (Figure 1D). Moreover, the combination of the liquid-based 3D culture system and stemness-enhancing medium significantly increased *Abcg2* gene expression.

These data indicated that 3D-cultured tumoroids with cancer stem phenotype were more platinum-resistant than 2D-cultured cancer cells. Larger tumoroids were more platinum-resistant than smaller cell aggregates. The 3D tumoroid formation of mCSC cells induced *Abcg2* expression that may involve Cisplatin efflux.

Preprints (www.preprints.org) | NOT PEER-REVIEWED | Posted: 23 December 2020 doi:10.20944/preprints202012.0582.v1

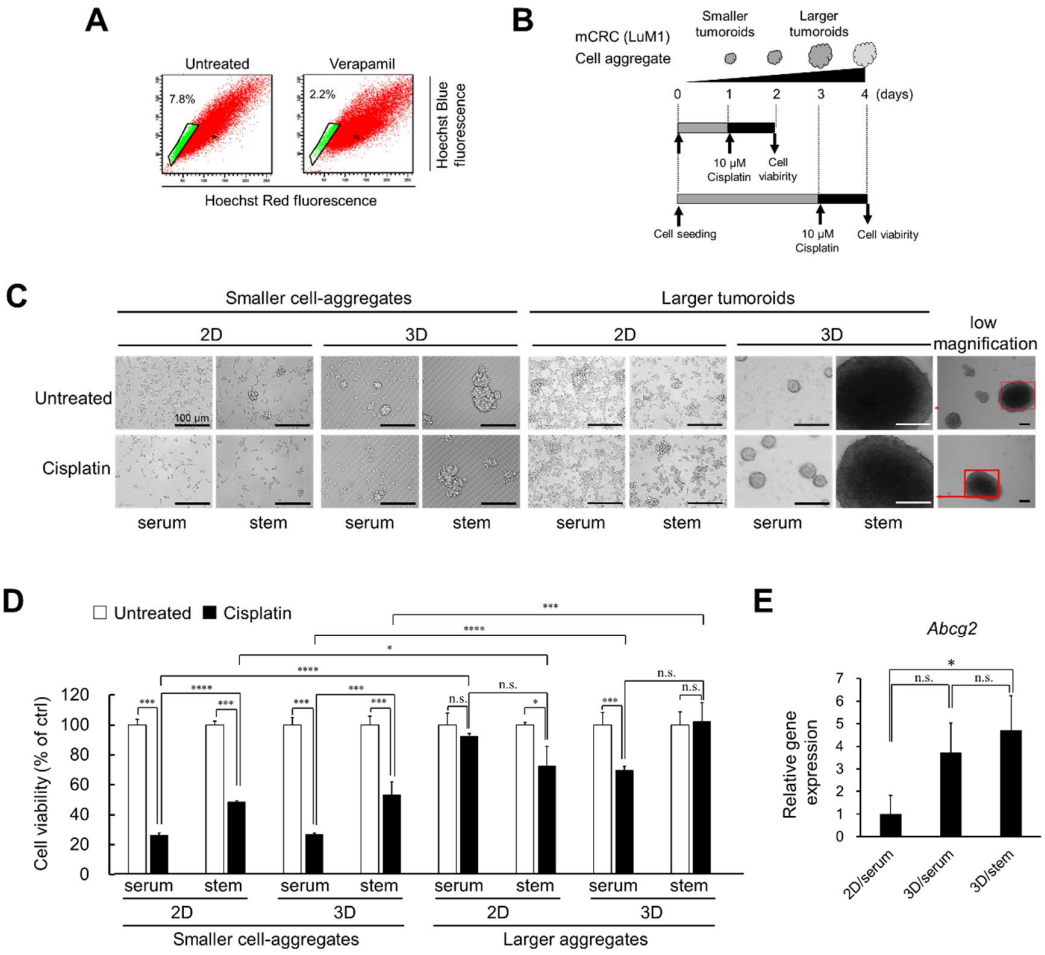

Figure 1. Tumoroids acquired platinum-resistance in metastatic colorectal cancer cells (mCRC). (**A**) Analysis of side population (SP) cells. LuM1 cells were treated with verapamil or untreated and then treated with Hoechst dye for flow cytometry. Green dots in the enclosed area indicate SP cells, whereas red dots are the main population cells. (B) Schemes of the experimental protocol. Smaller cell-aggregates were formed by pre-culturing LuM1 cells for 1 day. Larger tumoroids were formed by pre-culturing the cells for 3 days. Cisplatin at 10 μM was added to the tumoroids, and cell viability was measured. (**C**) Representative images of cells and tumoroids cultured in 2D vs. 3D culture plates. Cells were cultured serum-containing medium or mTeSR1 stem cell medium. Scale bars, 100 μm. (D) Cell viabilities of LuM1 cells and tumoroids treated with Cisplatin or untreated. n=3 or 4. (E) Gene expression of *Abcg2* in 2D vs. 3D culture conditions. n=4. *P<0.05, **P<0.01, ***P<0.001, ****P<0.0001, n.s., not significant.

3.2. Cisplatin promoted tumoroid formation of metastatic colorectal cancer

Next, we asked whether pre-formed, enlarged tumoroids were resistant to Cisplatin. Cisplatin did not alter viability and Mmp9 promoter activity in the mCRC LuM1 cells (Figure 2 A, B, C). Notably, Cisplatin tended to stimulate tumoroid growth (Figure 2D, 2E). The large tumoroids (10,000 to 20,000 μm^2) were formed by cisplatin treatment, which was not found in the untreated group (Figure 2F). Cisplatin treatment significantly increased the tumoroid size as compared with the untreated group (Figure 2G). These data indicated that the Cisplatin is ineffective to pre-formed, enlarged tumoroids, promoting rather tumoroid growth.

Next, we examined a lower concentration (2 μM) of Cisplatin altered tumoroid growth. Cisplatin at 2 μM significantly increased tumoroid size (Figure 2J), the rate of

Preprints (www.preprints.org) | NOT PEER-REVIEWED | Posted: 23 December 2020 doi:10.20944/preprints202012.0582.v1

large tumoroids > 300 μm² (Figure 2K), and Mmp9 promoter activity (Figure 2L). These data indicated that Cisplatin at 2 μM can promote tumor growth in mCRC cells.

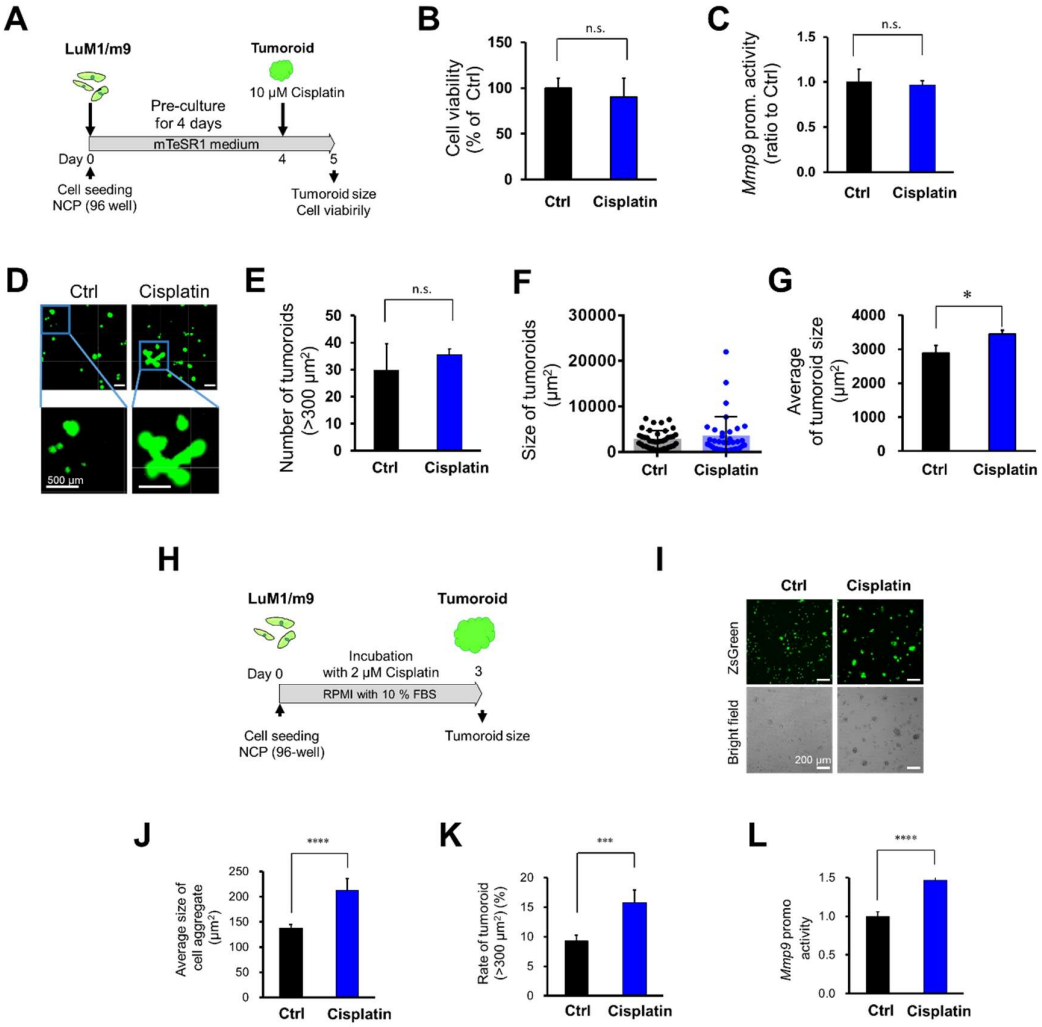

Figure 2. Cisplatin promoted tumoroid formation of mCRC cells. (**A**) A scheme of the experimental protocol used for panel B-G. LuM1/m9 cells were pre-cultured for 4 days in mTeSR1 on NCP, and then Cisplatin at 10 μM was added. (**B**) Cell viability. n=3 wells. (**C**) Mmp9 promoter activity. n=3 wells. (**D**) Representative images of tumoroids. Scale bars, 500 μm. (**E**) The number of tumoroids larger than 300 μm². n= 2 or 3 wells. (**F**) Column scatters plotting of tumoroid size. (**G**) average tumoroid size. n= 2 or 3 wells. (**H**) A scheme of the experimental protocol used for panel I-L. LuM1/m9 cells were cultured with 2 μM Cisplatin for 3 days in a medium containing 10% FBS. (**I**) Representative images of cell aggregates. Scale bars, 200 μm. (**J**) Average tumoroid size. n= 2 or 3 wells. (**K**) The number of tumoroids larger than 300 μm². n= 2 or 3 wells. (**L**) Mmp9 promoter activity. n= 2 or 3 wells. *P<0.05, **P<0.01, ***P<0.001, ****P<0.0001, n.s., not significant.

3.3. Imatinib promoted tumoroid growth of mCRC

Next, we examined whether Imatinib, a tyrosine kinase inhibitor, altered the tumoroid growth of mCRC cells. Imatinib (10 μM) significantly promoted tumoroid growth (Figure 3A, B, C). The rate of large tumoroids >300 μm² was significantly increased by imatinib treatment (Figure 3B). The size of tumoroids was also significantly increased by imatinib treatment (Figure 3C). The *Mmp9* promoter activity was significantly increased by

Preprints (www.preprints.org) | NOT PEER-REVIEWED | Posted: 23 December 2020 doi:10.20944/preprints202012.0582.v1

imatinib treatment. However, cellular viability was not altered by imatinib treatment (Figure 3E).

These data indicated that mCRC tumoroids of LuM1 were imatinib-resistant. Imatinib can promote cell aggregation and intercellular adhesion of mCRC cells.

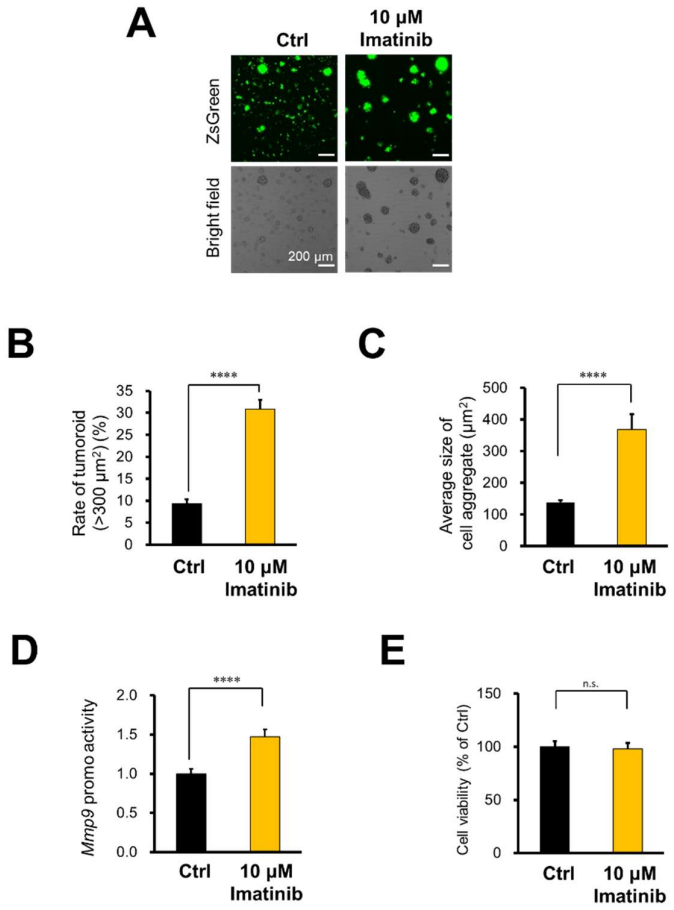

Figure 3. Imatinib promoted tumoroid growth of mCRC. LuM1/m9 cells were cultured with 10 μM Imatinib for 3 days in a medium containing 10% FBS. (A) Representative images of cell-aggregates with or without Imatinib. Scale bars, 200 μm. (B) The rate of tumoroids larger than 300 μm². n=4 wells. (C) The average size of cell aggregates or tumoroids. n=4 wells. (D) Mmp9 promoter activity. n=4 wells. (E) Cell viability. n= 4 wells. *P<0.05, **P<0.01, ***P<0.001, ****P<0.0001, n.s., not significant.

3.4. 5-FU inhibited tumoroid growth of mCRC, although not completely.

We next asked whether 5-FU, an antimetabolite against DNA replication, altered tumoroid growth of mCRC cells. 5-FU treatment significantly inhibited tumoroid growth of mCRC LuM1 in a concentration-dependent manner (Figure 4A, B, C). 5-FU (1 or 10 μM) significantly reduced large tumoroids >300 μm² in the concentration-dependent manner (Figure 4B). 5-FU (1 or 10 μM) significantly reduced the size of tumoroids in a concentration-dependent manner (Figure 4C). 5-FU (1 or 10 μM) significantly reduced cell viability of mCRC tumoroids in a concentration-dependent manner (Figure 4D). On the other hand, the *Mmp9* promoter activity in the survived cells was increased by 5-FU treatment (Figure 4E). Nevertheless, these data indicated that 5-FU is effectively cytotoxic to mCRC tumoroids, whereas survived 5-FU-resistant cells may involve relapse in mCRC.

Preprints (www.preprints.org) | NOT PEER-REVIEWED | Posted: 23 December 2020 doi:10.20944/preprints202012.0582.v1

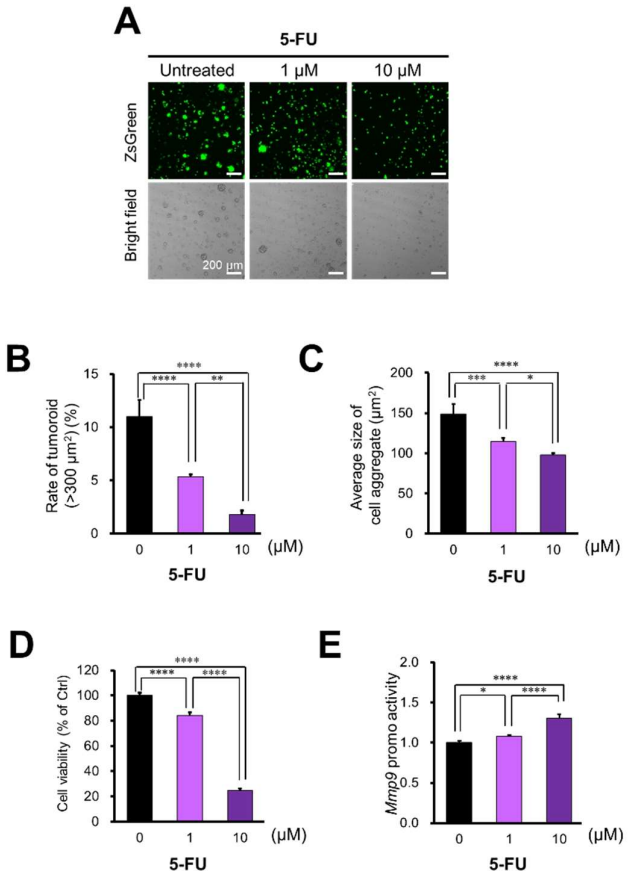

Figure 4. 5-FU inhibited tumoroid growth of mCRC, although not completely. LuM1/m9 cells were cultured with 5-FU at 0, 1, or 10 μM for 3 days in a medium containing 10% FBS. (A) Representative images of cell-aggregates of LuM1/m9. Scale bars, 200 μm². (B) The rate of tumoroids larger than 300 μm². n=4 wells. (C) The average size of cell aggregates. n=4 wells. (D) Cell viability. n=4 wells. (E) Mmp9 promoter activity. n=4 wells. *P<0.05, **P<0.01, ***P<0.001, ****P<0.0001, n.s., not significant.

4. Discussion

Drug resistance is an unsolved issue, especially in metastatic cancer, including mCRC. Many studies have examined chemoresistance in 2D culture systems, whereas our current study significantly demonstrated that the 3D culture system is a suitable, easily accessible tool to analyze drug resistance in metastatic cancer in vitro. Our study showed that Cisplatin (a platinum-based DNA crosslinker) and Imatinib (TKI) were ineffective and rather promote tumor growth of the metastatic CRC cells. On the other hand, 5-FU (an antimetabolite inhibiting DNA replication) more effectively combat the tumor growth of mCRC, although MMP9-positive metastatic cancer cells remained even after the 5-FU treatment, which was thought to be insensitive, dormant cancer cells in the tumoroids. Thus, the 3D tumoroid culture system is useful for further analyzing drug resistance and metastatic cancer cells' sensitivity.

Our study touch upon the mechanisms of platinum resistance using the liquid-based 3D tumoroid model. Tumoroid growth induces both ABCG2 expression (Figure 1) and exosome secretion [6,7,15]. Therefore, it is conceivable that Cisplatin could be secreted from cancer cells with exosomes and via ABC transporters such as ABCG2 efflux pump (Figure S2). Several studies showed that Cisplatin was secreted with exosomes from cancer cells [25,29,30]. Notably, we showed even anti-EGFR antibody-based drug (cetuximab)

 doi:10.20944/preprints202012.0582.v1

was secreted with exosomes from metastatic oral cancer cells [26]. Moreover, cancer cell-derived EVs, including exosomes, promote tumor growth of mCRC in vitro and in vivo [6,21]. Therefore, Cisplatin-induced exosomes may promote tumor growth, which may be a mechanism by which Cisplatin promoted tumor growth.

Our data showed that Imatinib was not cytotoxic but promoted tumoroid growth of mCRC. Imatinib is a TKI that can inhibit multiple TKs, including receptor tyrosine kinases (RTK), in cancer cells. c-Kit is one of the RTKs targeted by Imatinib. Chau et al. reported c-Kit mediated chemoresistance and tumor-initiating capacity of ovarian cancer cells through activation of Wnt/β-catenin-ABCG2 signaling [31]. Moreover, Imatinib was reported to upregulate compensatory integrin signaling in a mouse model of the gastrointestinal stromal tumor (GIST) [32]. It was also shown that Src family kinase induced Imatinib resistance in a kinase-dependent manner in chronic myelogenous leukemia (CML) cells [33]. Src family kinase has been shown to mediate growth factor signals to multiple pathways, including STAT, Ras-MEK-ERK, and PI3K-Akt [32,34]. Among these pathways, STAT3 is crucial for activating the *MMP9* gene and cancer stem phenotype in the 3D tumoroid model [13] (Figure S2).

Moreover, Liu et al. reported exosome release in Imatinib-resistant human CML cells [35]. Also, it has been reported that ABCG2 transports anticancer agents such as Imatinib from cells [24]. Therefore, it was suggested that the integrins-Src-STAT3 signaling pathway, exosome release, and/or efflux via ABCG2 may cause Imatinib resistance. The only hope is that tumoroid formation is associated with the inhibition of epithelial-to-mesenchymal transition (EMT) [3]. EMT involves the migratory, invasive, and metastatic ability of cancer cells [12,36], and thus inhibition of EMT is a potent strategy for cancer therapy. Tumoroid formation with intercellular adhesion is a result of an anti-EMT effect of the drugs. Imatinib may inhibit EMT and thus inhibit the invasive, metastatic ability of cancer cells.

It has been known that many chemotherapeutics unselectively kill proliferating cells, including cancer cells and myeloid, in patients and thus often cause adverse effects, including myelosuppression. These limitations in chemotherapies have been overcome by molecularly targeted drugs, including antibody-based drugs. Moreover, precision medicine has enabled precise diagnosis-based medications, e.g., if the mCRC was EGFR-positive and RAS-wildtype, anti-EGFR antibody drugs such as cetuximab would be effective for cancer. In the present study, we showed that the liquid-based 3D tumoroid assay is markedly useful to evaluate chemotherapeutics' drug efficacy, while presumably of antibody-based drugs as well. To study efficacies of antibody-based drugs, it is recommended to add effector immune cells such as killer T cells, natural killer cells, or macrophages that express Fc receptors and can exert antibody-dependent cellular cytotoxicity (ADCC) or antibody-dependent cellular phagocytosis (ADCP) [25,37,38]. Nevertheless, it is conceived that large tumoroids might be resistant to ADCC and ADCP. We are currently exploring tumoroid-based tumor immunology.

5. Conclusions

In conclusion, platinum resistance and imatinib resistance in metastatic colorectal cancer were modeled using the liquid-based 3D cultured tumoroid system. The 3D tumoroid system is useful and easily accessible for drug assessment, including chemosensitivity and chemoresistance.

Supplementary Materials: Figure S1: Side population (SP) cells were reduced by verapamil treatment in Colon26 cell line, Figure S2: Interpretation of data.

Author Contributions: Conceptualization, C.S. and T.E.; methodology, C.S., T.E. and E.A.; software, C.S.; validation, C.S. and Y.N.; formal analysis, C.S.; investigation, C.S. and Y.N.; resources, T.E. and C.S.; data curation, C.S. and T.E. ; writing—original draft preparation, C.S. and T.E.; writing—review and editing, T.E.; visualization, C.S. and T.E.; supervision, K.Ok.; project administration, C.S. and T.E.; funding acquisition, C.S., T.E., and K.Oh. All authors have read and agreed to the published version of the manuscript.

Funding: This research was funded by JSPS Kakenhi, grant number 20K09904 (C.S., T.E., K.Ok, and E.A.), 17K11669 (K.Oh., T.E., C.S.), Suzuken Memorial Foundation (T.E.), and Ryobi Teien Memorial Foundation (C.S.)

Institutional Review Board Statement: Not applicable.

Informed Consent Statement: Not applicable.

Acknowledgments: This paper is dedicated to the memory of Professor Ken-ichi Kozaki, who deceased on May 29, 2016.

Conflicts of Interest: The authors declare no conflict of interest.

References

1. Chou, S.D.; Murshid, A.; Eguchi, T.; Gong, J.; Calderwood, S.K. HSF1 regulation of beta-catenin in mammary cancer cells through control of HuR/elavL1 expression. *Oncogene* **2015**, *34*, 2178-2188, doi:10.1038/onc.2014.177.
2. Ishiguro, T.; Ohata, H.; Sato, A.; Yamawaki, K.; Enomoto, T.; Okamoto, K. Tumor-derived spheroids: Relevance to cancer stem cells and clinical applications. *Cancer Sci* **2017**, *108*, 283-289, doi:10.1111/cas.13155.
3. Arai, K.; Eguchi, T.; Rahman, M.M.; Sakamoto, R.; Masuda, N.; Nakatsura, T.; Calderwood, S.K.; Kozaki, K.; Itoh, M. A Novel High-Throughput 3D Screening System for EMT Inhibitors: A Pilot Screening Discovered the EMT Inhibitory Activity of CDK2 Inhibitor SU9516. *PLoS One* **2016**, *11*, e0162394, doi:10.1371/journal.pone.0162394.
4. Boj, S.F.; Hwang, C.I.; Baker, L.A.; Chio, II; Engle, D.D.; Corbo, V.; Jager, M.; Ponz-Sarvise, M.; Tiriac, H.; Spector, M.S., et al. Organoid models of human and mouse ductal pancreatic cancer. *Cell* **2015**, *160*, 324-338, doi:10.1016/j.cell.2014.12.021.
5. Takai, A.; Fako, V.; Dang, H.; Forgues, M.; Yu, Z.; Budhu, A.; Wang, X.W. Three-dimensional Organotypic Culture Models of Human Hepatocellular Carcinoma. *Sci Rep* **2016**, *6*, 21174, doi:10.1038/srep21174.
6. Taha, E.A.; Sogawa, C.; Okusha, Y.; Kawai, H.; Oo, M.W.; Elseoudi, A.; Lu, Y.; Nagatsuka, H.; Kubota, S.; Satoh, A., et al. Knockout of MMP3 Weakens Solid Tumor Organoids and Cancer Extracellular Vesicles. *Cancers (Basel)* **2020**, *12*, doi:10.3390/cancers12051260.
7. Eguchi, T.; Sogawa, C.; Okusha, Y.; Uchibe, K.; Iinuma, R.; Ono, K.; Nakano, K.; Murakami, J.; Itoh, M.; Arai, K., et al. Organoids with Cancer Stem Cell-like Properties Secrete Exosomes and HSP90 in a 3D NanoEnvironment. *PLOS ONE* **2018**, *13*, e0191109, doi:10.1371/journal.pone.0191109.
8. Nicolini, A.; Rossi, G.; Ferrari, P.; Carpi, A. Minimal residual disease in advanced or metastatic solid cancers: The G0-G1 state and immunotherapy are key to unwinding cancer complexity. *Semin Cancer Biol* **2020**, doi:10.1016/j.semcancer.2020.03.009.
9. Butturini, E.; Carcereri de Prati, A.; Boriero, D.; Mariotto, S. Tumor Dormancy and Interplay with Hypoxic Tumor Microenvironment. *Int J Mol Sci* **2019**, *20*, doi:10.3390/ijms20174305.
10. Walker, N.D.; Patel, J.; Munoz, J.L.; Hu, M.; Guiro, K.; Sinha, G.; Rameshwar, P. The bone marrow niche in support of breast cancer dormancy. *Cancer Lett* **2016**, *380*, 263-271, doi:10.1016/j.canlet.2015.10.033.
11. Senkowski, W.; Zhang, X.; Olofsson, M.H.; Isacson, R.; Hoglund, U.; Gustafsson, M.; Nygren, P.; Linder, S.; Larsson, R.; Fryknas, M. Three-Dimensional Cell Culture-Based Screening Identifies the Anthelmintic Drug Nitazoxanide as a Candidate for Treatment of Colorectal Cancer. *Mol Cancer Ther* **2015**, *14*, 1504-1516, doi:10.1158/1535-7163.MCT-14-0792.
12. Ono, K.; Sogawa, C.; Kawai, H.; Tran, M.T.; Taha, E.A.; Lu, Y.; Oo, M.W.; Okusha, Y.; Okamura, H.; Ibaragi, S., et al. Triple knockdown of CDC37, HSP90-alpha and HSP90-beta diminishes extracellular vesicles-driven malignancy events and macrophage M2 polarization in oral cancer. *J Extracell Vesicles* **2020**, *9*, 1-21, doi:10.1080/20013078.2020.1769373.
13. Sogawa, C.; Eguchi, T.; Tran, M.T.; Ishige, M.; Trin, K.; Okusha, Y.; Taha, E.A.; Lu, Y.; Kawai, H.; Sogawa, N., et al. Antiparkinson Drug Benztropine Suppresses Tumor Growth, Circulating Tumor Cells, and Metastasis by Acting on SLC6A3/DAT and Reducing STAT3. *Cancers (Basel)* **2020**, *12*, 1-22.
14. Sogawa, C.; Eguchi, T.; Okusha, Y.; Ono, K.; Ohyama, K.; Iizuka, M.; Kawasaki, R.; Hamada, Y.; Takigawa, M.; Sogawa, N., et al. A reporter system evaluates tumorigenesis, metastasis, beta-catenin/MMP regulation, and druggability. *Tissue Eng Part A* **2019**, *25*, 1413-1425, doi:10.1089/ten.TEA.2018.0348.
15. Namba, Y.; Sogawa, C.; Okusha, Y.; Kawai, H.; Itagaki, M.; Ono, K.; Murakami, J.; Aoyama, E.; Ohyama, K.; Asaumi, J., et al. Depletion of Lipid Efflux Pump ABCG1 Triggers the Intracellular Accumulation of Extracellular Vesicles and Reduces Aggregation and Tumorigenesis of Metastatic Cancer Cells. *Front Oncol* **2018**, *8*, 1-16, doi:10.3389/fonc.2018.00376.
16. Yoshida, S.; Kawai, H.; Eguchi, T.; Sukegawa, S.; Oo, M.W.; Anqi, C.; Takabatake, K.; Nakano, K.; Okamoto, K.; Nagatsuka, H. Tumor Angiogenic Inhibition Triggered Necrosis (TAITN) in Oral Cancer. *Cells* **2019**, *8*, 1-15, doi:10.3390/cells8070761.
17. Shimo, T.; Kubota, S.; Yoshioka, N.; Ibaragi, S.; Isowa, S.; Eguchi, T.; Sasaki, A.; Takigawa, M. Pathogenic role of connective tissue growth factor (CTGF/CCN2) in osteolytic metastasis of breast cancer. *J Bone Miner Res* **2006**, *21*, 1045-1059, doi:10.1359/jbmr.060416.
18. Drost, J.; Clevers, H. Translational applications of adult stem cell-derived organoids. *Development* **2017**, *144*, 968-975, doi:10.1242/dev.140566.
19. Karthaus, W.R.; Iaquinta, P.J.; Drost, J.; Gracanin, A.; van Boxtel, R.; Wongvipat, J.; Dowling, C.M.; Gao, D.; Begthel, H.; Sachs, N., et al. Identification of multipotent luminal progenitor cells in human prostate organoid cultures. *Cell* **2014**, *159*, 163-175, doi:10.1016/j.cell.2014.08.017.

20. Palikuqi, B.; Nguyen, D.T.; Li, G.; Schreiner, R.; Pellegata, A.F.; Liu, Y.; Redmond, D.; Geng, F.; Lin, Y.; Gomez-Salinero, J.M., et al. Adaptable haemodynamic endothelial cells for organogenesis and tumorigenesis. *Nature* **2020**, *585*, 426-432, doi:10.1038/s41586-020-2712-z.
21. Okusha, Y.; Eguchi, T.; Tran, M.T.; Sogawa, C.; Yoshida, K.; Itagaki, M.; Taha, E.A.; Ono, K.; Aoyama, E.; Okamura, H., et al. Extracellular Vesicles Enriched with Moonlighting Metalloproteinase Are Highly Transmissive, Pro-Tumorigenic, and Trans-Activates Cellular Communication Network Factor (CCN2/CTGF): CRISPR against Cancer. *Cancers (Basel)* **2020**, *12*, doi:10.3390/cancers12040881.
22. Okusha, Y.; Eguchi, T.; Sogawa, C.; Okui, T.; Nakano, K.; Okamoto, K.; Kozaki, K. The intranuclear PEX domain of MMP involves proliferation, migration, and metastasis of aggressive adenocarcinoma cells. *J Cell Biochem* **2018**, *119*, 7363-7376, doi:10.1002/jcb.27040.
23. Eguchi, T.; Taha, E.A. Extracellular Vesicle-associated Moonlighting Proteins: Heat Shock Proteins and Metalloproteinases. In *Heat Shock Proteins*, Asea, A.A.A., Kaur, P., Eds. Springer, Dordrecht: 2020; pp. 1-18.
24. Noguchi, K.; Katayama, K.; Sugimoto, Y. Human ABC transporter ABCG2/BCRP expression in chemoresistance: basic and clinical perspectives for molecular cancer therapeutics. *Pharmgenomics Pers Med* **2014**, *7*, 53-64, doi:10.2147/pgpm.S38295.
25. Eguchi, T.; Taha, E.A.; Calderwood, S.K.; Ono, K. A Novel Model of Cancer Drug Resistance: Oncosomal Release of Cytotoxic and Antibody-Based Drugs. *Biology (Basel)* **2020**, *9*, 1-22, doi:10.3390/biology9030047.
26. Fujiwara, T.; Eguchi, T.; Sogawa, C.; Ono, K.; Murakami, J.; Ibaragi, S.; Asaumi, J.; Okamoto, K.; Calderwood, S.K.; Kozaki, K. Anti-EGFR antibody cetuximab is secreted by oral squamous cell carcinoma and alters EGF-driven mesenchymal transition. *Biochem Biophys Res Commun.* **2018**, *503*, 1267-1272.
27. Sakata K; Kozaki K; Iida K; Tanaka R; Yamagata S; Utsumi KR; Saga S; Shimizu S; Matsuyama, M. Establishment and characterization of high- and low-lung-metastatic cell lines derived from murine colon adenocarcinoma 26 tumor line. *Jpn J Cancer Res (Cancer Sci)* **1996**, *87*, 78-85.
28. Namba, Y.; Sogawa, C.; Okusha, Y.; Kawai, H.; Itagaki, M.; Ono, K.; Murakami, J.; Aoyama, E.; Ohyama, K.; Asaumi, J.I., et al. Depletion of Lipid Efflux Pump ABCG1 Triggers the Intracellular Accumulation of Extracellular Vesicles and Reduces Aggregation and Tumorigenesis of Metastatic Cancer Cells. *Front. Oncol.* **2018**, *8*, 376, doi:10.3389/fonc.2018.00376.
29. Safaei, R.; Larson, B.J.; Cheng, T.C.; Gibson, M.A.; Otani, S.; Naerdemann, W.; Howell, S.B. Abnormal lysosomal trafficking and enhanced exosomal export of Cisplatin in drug-resistant human ovarian carcinoma cells. *Mol Cancer Ther* **2005**, *4*, 1595-1604, doi:10.1158/1535-7163.Mct-05-0102.
30. Yin, J.; Yan, X.; Yao, X.; Zhang, Y.; Shan, Y.; Mao, N.; Yang, Y.; Pan, L. Secretion of annexin A3 from ovarian cancer cells and its association with platinum resistance in ovarian cancer patients. *Journal of cellular and molecular medicine* **2012**, *16*, 337-348, doi:10.1111/j.1582-4934.2011.01316.x.
31. Chau, W.K.; Ip, C.K.; Mak, A.S.; Lai, H.C.; Wong, A.S. c-Kit mediates chemoresistance and tumor-initiating capacity of ovarian cancer cells through activation of Wnt/beta-catenin-ATP-binding cassette G2 signaling. *Oncogene* **2013**, *32*, 2767-2781, doi:10.1038/onc.2012.290.
32. Rossi, F.; Yozgat, Y.; de Stanchina, E.; Veach, D.; Clarkson, B.; Manova, K.; Giancotti, F.G.; Antonescu, C.R.; Besmer, P. Imatinib upregulates compensatory integrin signaling in a mouse model of gastrointestinal stromal tumor and is more effective when combined with dasatinib. *Mol Cancer Res* **2010**, *8*, 1271-1283, doi:10.1158/1541-7786.MCR-10-0065.
33. Pene-Dumitrescu, T.; Smithgall, T.E. Expression of a Src family kinase in chronic myelogenous leukemia cells induces resistance to Imatinib in a kinase-dependent manner. *J Biol Chem* **2010**, *285*, 21446-21457, doi:10.1074/jbc.M109.090043.
34. Larue, L.; Bellacosa, A. Epithelial-mesenchymal transition in development and cancer: role of phosphatidylinositol 3' kinase/AKT pathways. *Oncogene* **2005**, *24*, 7443-7454, doi:10.1038/sj.onc.1209091.
35. Liu, J.; Zhang, Y.; Liu, A.; Wang, J.; Li, L.; Chen, X.; Gao, X.; Xue, Y.; Zhang, X.; Liu, Y. Distinct Dasatinib-Induced Mechanisms of Apoptotic Response and Exosome Release in Imatinib-Resistant Human Chronic Myeloid Leukemia Cells. *International journal of molecular sciences* **2016**, *17*, 531-531, doi:10.3390/ijms17040531.
36. Fujiwara, T.; Eguchi, T.; Sogawa, C.; Ono, K.; Murakami, J.; Ibaragi, S.; Asaumi, J.; Calderwood, S.K.; Okamoto, K.; Kozaki, K. Carcinogenic epithelial-mesenchymal transition initiated by oral cancer exosomes is inhibited by anti-EGFR antibody cetuximab. *Oral Oncology* **2018**, *86*, 251-257, doi:10.1016/j.oraloncology.2018.09.030.
37. Braig, F.; Kriegs, M.; Voigtlaender, M.; Habel, B.; Grob, T.; Biskup, K.; Blanchard, V.; Sack, M.; Thalhammer, A.; Ben Batalla, I., et al. Cetuximab Resistance in Head and Neck Cancer Is Mediated by EGFR-K521 Polymorphism. *Cancer Res* **2017**, *77*, 1188-1199, doi:10.1158/0008-5472.CAN-16-0754.
38. Stangl, S.; Gehrmann, M.; Riegger, J.; Kuhs, K.; Riederer, I.; Sievert, W.; Hube, K.; Mocikat, R.; Dressel, R.; Kremmer, E., et al. Targeting membrane heat-shock protein 70 (Hsp70) on tumors by cmHsp70.1 antibody. *Proceedings of the National Academy of Sciences of the United States of America* **2011**, *108*, 733-738, doi:10.1073/pnas.1016065108.